Int. J. Electrochem. Sci., 14 **(2019)** 4946 – 4956, doi: 10.20964/2019.06.28

International Journal of ELECTROCHEMICAL SCIENCE
www.electrochemsci.org

Electrochemical Determination of Rutin Using SnO_2/nitrogen-doped Graphene Composite Electrode

Yingqiong Peng[1,], MuXin Liao[2], Xue Ma[3], Hong Deng[1], Feng Gao[3], Runying Dai[3,*], Limin Lu[3,*]*

[1] Colleges and Universities of Jiangxi Province for Key Laboratory of Information Technology in Agriculture, Software Institute, Jiangxi Agriculture University, Nanchang 330045, PR China
[2] College of Computer and Information Engineering, Jiangxi Agriculture University PR China,
[3] College of Science, Jiangxi Agricultural University, Nanchang 330045, PR China
[*]E-mail: jneyq_pyq@163.com, runyingdai@163.com, lulimin816@126.com

Received: 7 February 2019 / *Accepted:* 28 March 2019 / *Published:* 10 May 2019

Herein, the nanocomposites of SnO_2 nanoparticles on the nitrogen-doped graphene (SnO_2/NG) as a sensitive electrochemical sensing platform for rutin determination were easily prepared via a facile hydrothermal method. The results showed that the existence of NG in SnO_2/NG composites could dramatically improve the conductivity, facilitate the electron transfer and enhance the electro-catalytic activity of rutin. Compared with pure SnO_2, NG and SnO_2/graphene, the as-prepared SnO_2/NG nanocomposite presented improved electrocatalytic activity for the oxidation of rutin due to the synergetic effects from SnO_2 and NG. Combined with differential pulse voltammetry, the prepared sensor based on SnO_2/NG modified electrode displayed a wide linear range from 0.4 nM to 2 μM with a detection limit of 0.2 nM. The modified electrode exhibited high stability and reproducibility as well as good selectivity. These results suggest that SnO_2/NG could be successfully applied for detecting rutin in practical samples.

Keywords: SnO_2 nanoparticles; Nitrogen-doped graphene; rutin; Electrochemical determination

1. INTRODUCTION

Rutin is a biologically active flavonoid compound with a series of pharmacological and physiological effects such as anti-oxidant, anti-tumor and anti-inflammatory [1-2]. At present, a variety of analytical methods, including high performance liquid chromatography, spectrophotometry, capillary electrophoresis, chemiluminescence and electrochemical methods [3-7], have been applied to detect rutin. As for the electroactivity of rutin, electrochemical technique has been recognized as an effective strategy for the determination of rutin owing to its simplicity, high sensitivity and less

expensive instruments. Generally, electrochemical sensors need to use appropriate materials to modify the electrodes to enhance electrochemical properties such as sensitivity, selectivity and stability.

Metal oxide nanocrystals are of intense interests in material research and electrochemistry and have become one of the most interesting topics by virtue of their remarkable optical, electronic, and catalytic properties. These metal oxide nanomaterials show a brilliant prospect, but their practical applications are seriously hindered by their low intrinsic electrical conductivity and severe particle aggregation [8,9]. In view of the above problems, intensive research has been focused on compositing metal oxide with carbon based materials (fullerenes, carbon nanotubes, graphene, etc.) to achieve better electrochemical performance [10-12]. In particular, graphene has been recognized as an excellent support for catalysts loading on account of its superior physical and chemical properties. However, graphene sheets tend to stack together owing to their strong Van Der Waals force and π–π interactions [13], leading to decreased performance of metal oxide/graphene nanocomposites performance. Furthermore, the weak bonding between metal oxide nanoparticles and graphene support will also influence their efficiency [14]. Therefore, an appropriate carrier which can improve the dispersion, conductivity and enhance the catalytic activity from metal oxide nanoparticles is highly demanded.

Currently, nitrogen-doped graphene (NG), a novel carbonaceous-derived material, has attracted enormous attention because of its unique properties, including large surface active group to volume ratio, excellent biocompatibility, good electrical conductivity and a high density of active catalytic sites [15]. In addition, recent reports suggested that the incorporation of N dopants in graphene not only displays high binding affinities for metals and metal oxides by means of the nitrogen–metal (N–M) bond, but also improves their catalytic activities [16]. For example, Jiang et al. [17] synthesized Cu nanoparticles decorated NG (Cu/NG) via a facile thermal treatment and the obtained Cu/NG composite showed significant electrocatalytic activity to glucose oxidation. Balamurugan et al. [18] obtained a non-enzymatic NADH sensor based on iron nitride nanoparticles-encapsulated NG (FeN/NG). The proposed sensor showed much higher current than than of FeN and NG.

As a typical semiconductor, SnO_2 nanostructures with various morphologies has been designed and applied in many fields for its diverse optical, electrical and electrochemical properties, including gas sensor [19], catalysis [20] and Li ion battery [21]. In addition, there have been few reports about the preparation of SnO_2/NG composites and their application is limited in rechargeable lithium battery [22,23]. However, as far as we know, neither SnO_2 nor SnO_2/NG nanocomposites have been found in rutin detection. In this work, SnO_2/NG nanocomposites modified glassy carbon electrode (GCE) has been fabricated to study the electrochemical behavior of rutin for the first time. The combination of NG with SnO_2 can induce synergy between two components and demonstrate the enhanced property. Electrochemical analysis showed that the composite displayed superior electrocatalytic activity for rutin detection with a wide linear range and low detection limit. The designed sensor was further applied for actual sample analysis.

2. MATERIALS AND METHODS

2.1 Reagents

$SnCl_4 \cdot 5H_2O$ and ethylenediamine were bought from Sigma Chemical (USA). Graphene oxide was supplied by Nanjing Xianfeng Nanomaterials Technology Co. Ltd. (Nanjing, China). Britton Robinson (BR) buffer solutions of different pH values were used as working buffer. Other reagents of analytical grade. Distilled water was used in all experiments.

2.2 Apparatus

The TEM images were examined with transmission electron microscopy (G2 20, FEI Co., Ltd., USA). X-ray photoelectron spectra (XPS) was obtained by a K-Alpha spectrometer with a monochromatic Al Kα source (Thermo Fisher Scientific Inc., Switzerland). The cyclic voltammetric and differential pulse voltammetric measurements were performed on electrochemical workstation (CHI660E, ChenHua Instruments Co., Shanghai, China) using a conventional three-electrode system. A saturated calomel electrode (SCE) was used as a reference electrode. A platinum electrode served as counter electrode. A bare GCE (Φ = 3 mm) or modified GCE acted as the working electrode. All potentials were compared to SCE, and the entire experiments were operated at room temperature.

2.3 Preparation of SnO_2/NG nanocomposite

The SnO_2/NG nanocomposite was obtained using a previously reported procedure with minor modification [23]. Briefly, adding 0.5 g $SnCl_4 \cdot 5H_2O$ into GO aqueous solution (40 mL, 1 mg mL^{-1}), stirred for 10 min. Following that, 0.5 mL ethylenediamine (EDA) was dropped into the mixed solution. After stirring for another 10 min at ambient conditions, the mixture was poured into a Teflon-lined stainless steel autoclave and hydrothermally reduced at 180 °C for 24 h. Finally, the SnO_2/NG nanocomposite was centrifuged and washed with water and ethanol. Similarly, the pristine SnO_2, nitrogen-doped graphene and SnO_2/graphene were prepared in addition to adding GO, $SnCl_4 \cdot 5H_2O$ or ethylenediamine.

2.4 Construction of modified electrodes

GCE was carefully treated to a mirror-like plane with 0.3 μm and 0.05 μm Al_2O_3 slurries. After ultrasonic treatment in double distilled water, the GCE was dried under N_2 gas.

1.0 mg mL^{-1} SnO_2/NG suspension was obtained by dispersing 1.0 mg SnO_2/NG in 1.0 mL double distilled water under sonication for 30 min. After that, 5.0 μL of SnO_2/NG dispersion was dropped on the GCE surface and dried under an infrared lamp to form SnO_2/NG/GCE (Scheme 1). For comparison, bare GCE, SnO_2/GCE, NG/GCE and SnO_2/graphene/GCE were fabricated using the similar procedure.

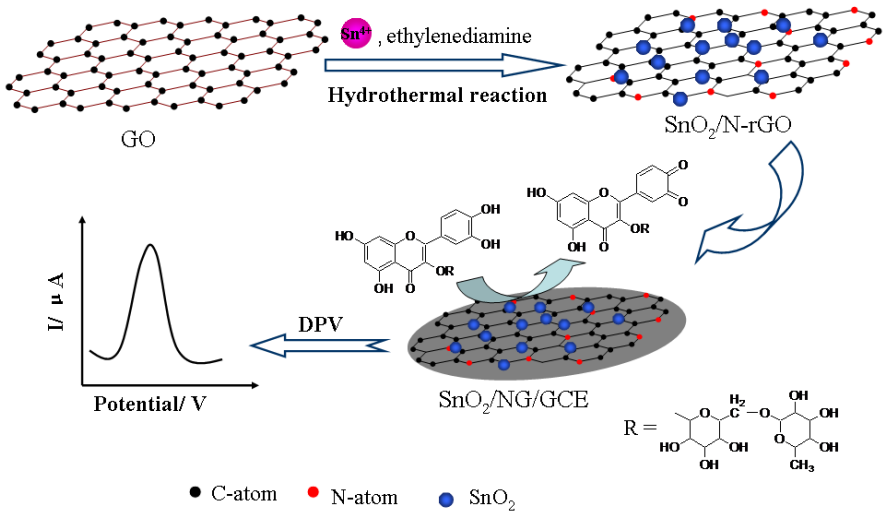

Scheme 1. Schematic illustration of the fabrication procedure of SnO_2/NG modified electrode.

3. RESULTS AND DISCUSSION

3.1 Materials characterization

Transmission electron microscopy (TEM) was used for characterizing the size, morphology and structure of the obtained materials. Figure 1A displayed that SnO_2 nanocrystallites were well-distributed on the graphene sheet's surface. Moreover, from the HRTEM image (Figure 1B), the average size of SnO_2 nanoparticles was 3–5 nm. Here, graphene oxide (GO) and EDA played important roles for the formation of the ultrasmall SnO_2 nanoparticles. GO has a plurality of oxygen-containing functional groups such as epoxy group, hydroxyl group and carboxylic acid group, which can form electrostatic interaction with Sn^{4+} and provides anchoring sites for Sn^{4+} [24]. On the other hand, EDA as a powerful complexing agent can form stable complexes with Sn^{4+}, which could decrease the hydrolysis reactivity of Sn^{4+}. The well-distributed SnO_2 nanoparticles on the NG with a high density could ensure excellent electrochemical properties and high stability of SnO_2/NG.

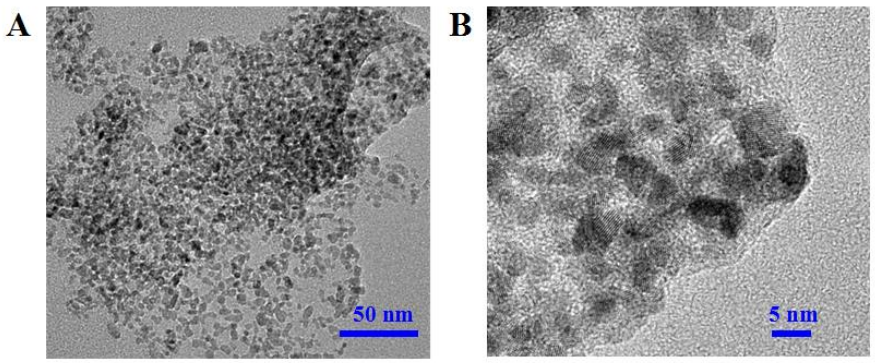

Figure 1. (A) TEM images of SnO_2/NG nanocomposites and (B) HRTEM image of SnO_2/NG nanocomposites.

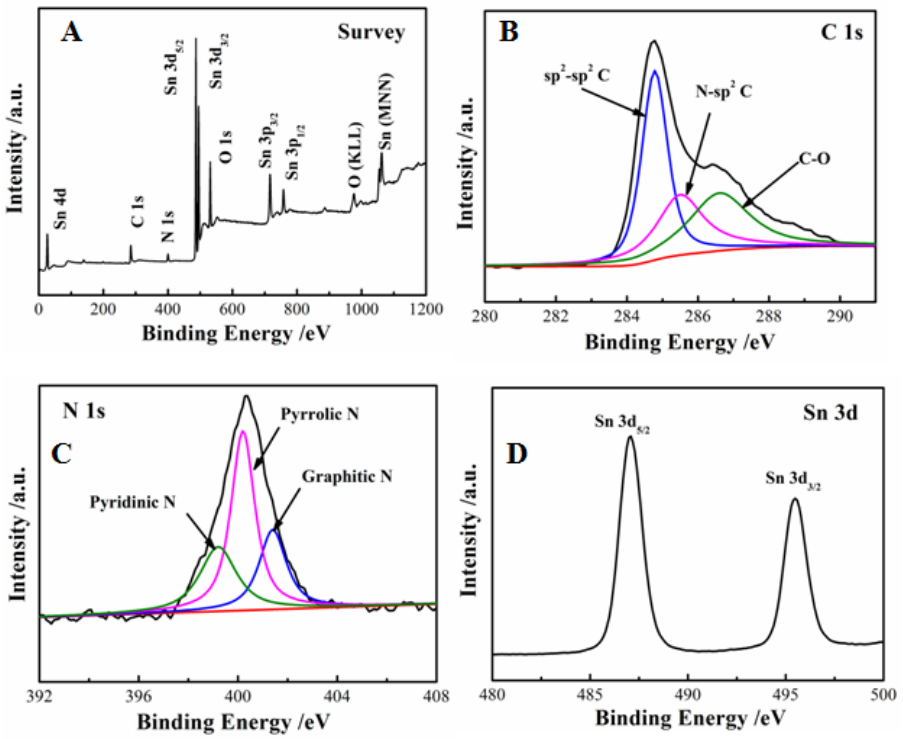

Figure 2. (A) XPS survey scan, (B) C 1s spectrum, (C) N 1s spectrum and (D) Sn 3d spectrum of SnO_2/NG nanocomposites.

The chemical composition of SnO_2/NG nanocomposites was investigated using XPS. Figure 2A demonstrated there were C, N, O, and Sn elements existence in the sample. The spectrum of C 1s (Figure 2B) displayed three peaks at 284.8, 285.5 and 286.6 eV, which corresponded to sp^2-sp^2 C, N-sp^2 C and C-O type bonds, respectively. In the spectrum of N 1s (Figure 2C), three well-resolved peaks located at 399.2, 400.2 and 401.4 eV, which were composed of pyridine nitrogen, pyrrole nitrogen and graphitized nitrogen atoms [23]. Figure 2D showed the high-resolution spectrum of Sn 3d, it can be seen that the two characteristic peaks appeared at 487 and 495.5 eV, respectively, which could be ascribed to the 3d 5/2 and 3d 3/2 of Sn (IV), indicating the existence of SnO_2 nanocrystallites in the nanocomposites [25].

3.2 Electrochemical property of rutin on different electrodes

Figure 3 displayed the cyclic voltammograms of 0.8 μM rutin on various modified electrodes in BR buffer solution (0.04 M, pH 2.0). A pair of weak redox peak currents appeared at bare GCE, observed from the curve a. For SnO_2/GCE (curve b), it showed a slight increase in redox peak currents comparing with bare GCE. By comparison, the oxidation peak value of rutin on NG/GCE (curve c) were dramatically enhanced, indicating NG possessed excellent electrical conductivity to improve the electron transfer rate and showed high electrocatalytic ability for the redox of rutin. Owing to the synergetic effects of NG and SnO_2, further enhancements in peak currents were observed at SnO_2/NG/GCE (curve e). Besides, it should be highlighted that the currents of the redox peaks on SnO_2/NG/GCE were obvious higher than that on SnO_2/graphene/GCE (curve d). These results indicate

that nitrogen doping in graphene can effectively change the electronic properties and accelerate the electron transfer of rutin [26,27]. Meanwhile, SnO_2/NG with large specific surface was beneficial for *accumulating* more rutin.

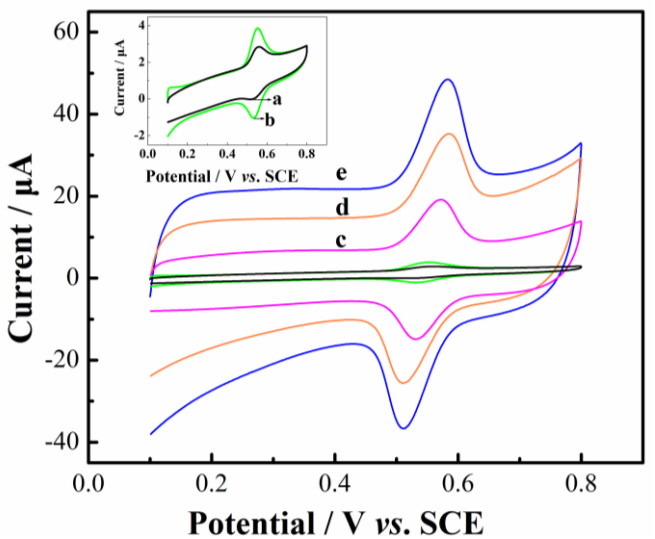

Figure 3. Cyclic voltammograms of 0.8 μM rutin in BR buffer solution (0.04 M, pH 2.0) on (a) bare GCE, (b) SnO_2/GCE, (c) NG/GCE, (d) SnO_2/graphene/GCE and (e) SnO_2/NG/GCE. Scan rate: 100 mV s^{-1}.

3.3 Optimization of the detection condition

3.3.1 pH effect

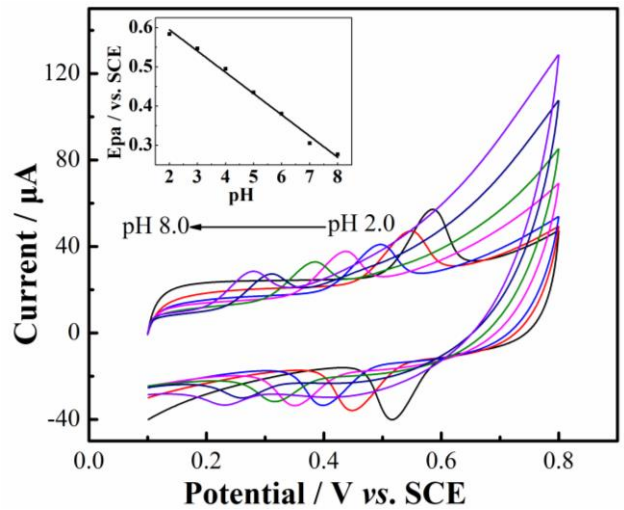

Figure 4. The pH influence of the solution in BR buffer solution (0.04 M) containing 0.9 μM rutin with pH 2.0-8.0 at SnO_2/NG/GCE. Scan rate: 100 mV s^{-1}. Inset: variation of peak potential vs. pH.

The effect of different pH values (0.04 M BR buffer solutions) on the electrochemical response of 0.9 μM rutin at SnO_2/NG/GCE was investigated. As shown in Figure 4, when the pH was increased from 2.0 to 8.0, both the anode peak and the cathode peak moved in the negative direction, implying that the proton participated in the electrochemical oxidation process. A good linearity of the anodic peak potential and pH value was obtained and the linear regression equation can be expressed as Epa/V = 0.7118–0.054 pH (R^2 = 0.9956) (inset of Figure 4). The slope value of -57 mV/pH was closed to the theortical value of -59 mV/pH, indicating that the number of electrons and protons participated in the electrode reaction was same [28, 29]. Furthermore, the oxidation peak current reached a maximum at pH 2.0. Therefore, the buffer solution pH of 2.0 was selected as the optimal condition in this work.

3.3.2 Accumulation time effect

Figure 5 displays the accumulation time effect, with the range from 60s to 450 s on the oxidation peak current of 0.4 μM rutin. The oxidation peak current increased obviously with the prolongation of accumulation time and reached a maximum at 200 s, which implied that the adsorption equilibrium was reached on SnO_2/NG/GCE. Thus, 200 s accumulation time was chosen as the optimum in further experiments.

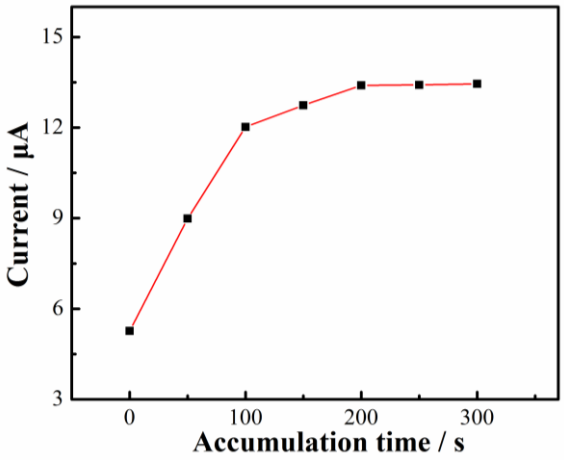

Figure 5. Influence of the accumulation times of 0.4 μM rutin on the oxidation peak current at SnO_2/NG/GCE in BR buffer solution (0.04 M, pH 2.0).

3.3.3 Scan rates effect

The influence of various scan rates on the redox behavior of rutin at SnO_2/NG/GCE was shown in Figure 6. With the increase of scanning rate from 20 mV/s to 300 mV/s, both the anodic (Ipa) and cathodic (Ipc) peak currents increased as the change of the redox peaks potentials. The corresponding linear relation between the anode (Epa) and cathode (Epc) peak currents and scan rate were found to

be: Ipa (μA) = 252.43 υ + 5.9446 (R^2= 0.99946) and Ipc (μA) = -220.47 υ - 2.2901 (R^2= 0.99952). These indicated that oxidation of rutin was an adsorption control process on the electrode surface [30].

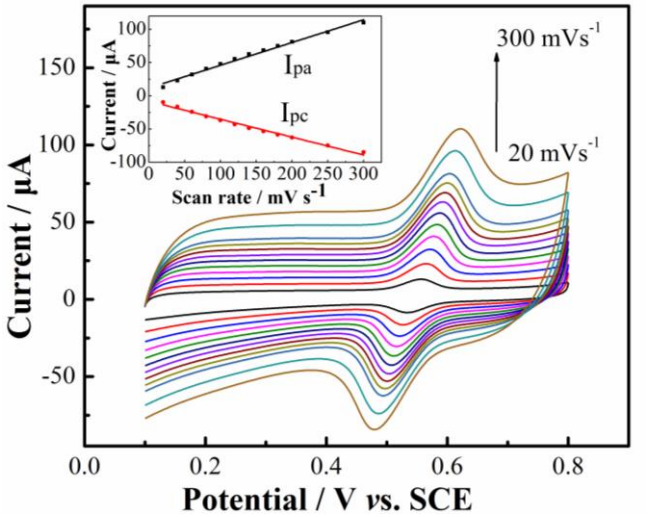

Figure 6. Cyclic voltammograms at SnO_2/NG/GCE in BR buffer solution (0.04 M, pH 2.0) containing 0.8 μM rutin with varying scan rates from 20 mV s^{-1} to 300 mV s^{-1}. Inset: plots of the anodic and cathodic peak currents *vs.* scan rate.

3.4 Analytical property of SnO_2/NG/GCE

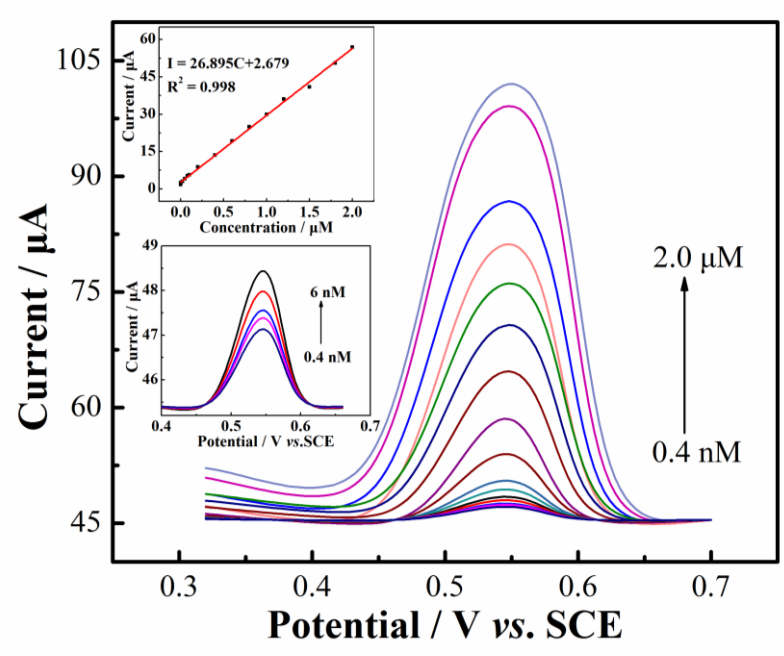

Figure 7. Differential pulse voltammetry curves of SnO_2/NG/GCE in BR buffer solution (0.04 M, pH 2.0) with different concentrations of rutin. Inset: calibration curve and DPV responses for rutin from 0.4 nM to 6.0 nM.

Under the optimal conditions, the analytical property of the SnO_2/NG/GCE for detection of rutin was researched by differential pulse voltammetry (DPV). The anodic peak currents increased

with increasing the concentrations of rutin as shown in Figure 7. The inset in Figure 7 showed that a linear calibration curve was observed from 0.4 nM to 2.0 μM. The corresponding equation was Ipa (μA) = 26.895C (μM) + 2.679 (R^2 = 0.9994). The low detection limit of 0.2 nM was acquired (S/N = 3). Table 1 displayed a comparison with the previously work [30-35]. The low detection limit of SnO_2/NG/GCE can be attributed to the favorable electron transfer and satisfactory electro-catalytic activity endowed by NG and SnO_2.

Table 1. Comparison of the performances of various rutin sensors

Electrodes	Linear range	Determination Limit	Reference
Ferrocene/AuNPs/graphene -chitosan/GCE	40 nM–100 μM	10 nM	[31]
β-cyclodextrin@chemically reduced graphene/GCE	6 nM – 10.0 μM	2 nM	[32]
carbon-coated nickel nano-particles/GCE	2 nM –1.72 μM	0.6 nM	[33]
AuNPs/CNT/carbon paste electrode	4 nM–1.0 μM	0.4 nM	[34]
Graphene-MnO_2/carbon ionic liquid electrode	10 nM – 500.0 μM	2.7 nM	[35]
NG/carbon ionic liquid electrode	7 nM – 10.0 μM	0.23 nM	[36]
SnO_2/NG/GCE	0.4 nM – 2 μM	0.2 nM	This work

3.5 Reproducibility, stability and selectivity of SnO_2/NG/GCE

The reproducibility of the SnO_2/NG/GCE was studied by repeated detection of 1.0 μM rutin. The relative standard deviation (RSD) was 3.2% (n= 5), meaning that the admirable reproducibility of the prepared sensor. To evaluate the stability of the electrode, SnO_2/NG/GCE was stored at room temperature for 20 days. For 1.0 μM rutin, the peak current of the anode was reduced less than 5% compared with the original value, indicating that the proposed sensor has favorable stability.

Interfering experiments are also indispensable for detection of rutin. A fixed amount of 1.0 μM rutin was mixed with various alien species. The results showed that NO_3^-, Cl^- and SO_4^{2-} in a 100-fold concentration, Na^+, K^+, Zn^{2+}, Ca^{2+} and Mg^{2+} in a 50-fold concentration, glucose and uric acid in a 10-fold concentration, the relative error was <±8%, it indicated that the electrochemical response of rutin has no obvious interference.

3.6. Analytical application

To test the feasibility and validity of the SnO_2/NG/GCE sensor, a standard addition method was used to measure the recovery of rutin in urine samples. As illustrated in Table 2, the recoveries obtained in diluted (100-fold) urine samples varied from 95.4% to 103.1%. The results from our designed method are in good agreement with high performance liquid chromatography (HPLC)

method. As expected, the fabricated sensor can be successfully applied for the determination of rutin in actual sample analysis.

Table 2. Determination of rutin in urine samples (n = 3)

Samples	Added (μM)	Founded (μM)	Recovery (%)	RSD (%)	by HPLC method
urine samples	0.0500	0.0515	104.0	4.4	0.0490
	0.5000	0.5025	100.5	3.6	0.5015
	1.0000	0.9770	97.7	2.8	0.9987

4. CONCLUSIONS

In this work, the SnO_2/NG nanocomposite was prepared by a simple method via thermal treatment, and a new electrochemical sensor for detecting rutin was constructed by using the resulting SnO_2/NG. The composite exhibited improved electrocatalytic activity to rutin oxidation than pure SnO_2, NG and SnO_2/graphene, which can be attributed to the introduction of nitrogen in graphene, the high dispersion of SnO_2 on NG, and the synergistic effect between SnO_2 and NG. The proposed approach displayed wide linear range from 0.4 nM to 2 μM with a detection limit 0.2 nM. In addition, the SnO_2/NG/GCE exhibited good reproducibility and stability, making SnO_2/NG nanocomposite a promising candidate for practical applications in the fields of detecting rutin.

ACKNOWLEDGEMENTS
We are grateful to the National Natural Science Foundation of China (21665010, 51862014, 31741103, 51302117), the special fund for visiting scholars in the development plan of young and middle-aged teachers in Jiangxi normal undergraduate universities (Jiangxi education organization letter [2016] 109), Jiangxi province science and technology support project (20123BBF60177), department of Education Science & Technology Program of Jiangxi Province (Grant NO. GJJ150405) for their financial support of this work.

References

1. S.Y. Park, S.H. Bok, S.M. Jeon, Y.B. Park, S.J. Lee, T.S. Jeong, *Nutr. Res.*, 22 (2002) 283.
2. R. Guo, P. Wei, *Microchim. Acta*, 161 (2008) 233.
3. Q.H. Lu, C.D. Ba, D.Y. Chen, *Pharm. Biomed. Anal*., 47 (2008) 888.
4. C.H. Wang, Y.X. Wang, H.J. Liu, *J. Pharm. Anal*., 1 (2011) 291.
5. Z. Cai, J. Zhao, C.Y. Jang, X.Y. Liang, L.S. Mo, *Chin. Pharm*., 20 (2009) 2454.
6. D. Yang, H. Li, Z. Li, Z. Hao, J. Li, *Luminescence*, 25 (2010) 436.
7. S.M. Li, B.B. Yang, J.Wang, D. Bin, C.Q. Wang, K. Zhang, Y.K. Du, *Anal. Methods*, 8 (2016) 5435.
8. L.H. Jiang, M.G. Yao, B. Liu, Q.J. Li, R. Liu, H. Lv, S.C. Lu, C. Gong, B. Zou, T. Cui, B.B. Liu, J. *Phys. Chem.* C., 116 (2012) 11741.
9. D. Jiang, X.J. Du, Q. Liu, L. Zhou, J. Qian, K. Wang, *ACS Appl. Mater. Interfaces*, 7 (2015) 3093.

10. T. Song, J.P. Huo, T. Liao, J. Zeng, J.Y. Qin, H.P. Zeng, *Eng. J*., 287 (2016) 359.
11. G.F. Huang, F. Zhang, X.C. Du, Y.L. Qin, D.M. Yin, L.M. Wang, *ACS Nano,* 9 (2015) 1592.
12. X.Y. Zhou, J.J. Shi, Y. Liu, Q.M. Su, J. Zhang, G.H. Du, *Electrochim. Acta,* 143 (2014) 175.
13. L. Meng, Y. Xia, W. Liu, L. Zhang, P.Zou, Y. Zhang, *Electrochim. Acta,* 152 (2015) 330.
14. X. Wang, X. Cao, L. Bourgeois, H. Guan, S. Chen, Y. Zhong, D.M. Tang, H. Li, T. Zhai, L. Li, Y. Bando, D. Golberg, *Funct. Mater.*, 22 (2012) 2682.
15. Y.Y. Chu, J. Cao, Z. Dai, X.Y. Tan, *J. Mater. Chem. A.,* 2 (2014) 4038.
16. Y. Wang, Y.Shao, D.W. Li, J. Matson, Y. Lin, *ACS Nano,* 4 (2010) 1790.
17. D. Jiang, Q. Liu, K. Wang, Z.T. Yang, X.J. Du, B.J. Qiu, *Biosens. Bioelectron.*, 54 (2014) 273.
18. J. Balamurugan, T.D. Thanh, N.H. Kim, J.H. Lee, *Biosens. Bioelectron.*, 83 (2016) 68.
19. Q. Kuang, C.S. Lao, Z.L. Wang, Z.X. Xie, L.S. Zheng, *J. Am. Chem. Soc.*, 129 (2007) 6070.
20. N. Lavanya, S. Radhakrisnan, N. Sudhan, C. Sekar, S.G. Leonardi, C. Cannilla, G. Neri, *Nanotechnology,* 25 (2014) 295501.
21. Z.Y. Wang, D.Y. Luan, F.Y. Boey, X.W. Lou, *J. Am. Chem. Soc.*, 133 (2011) 4738.
22. J.F. Liang, Z. Cai, Y. Tian, L.D. Li, J.X. Geng, L. Guo, *Mater. Interfaces,* 5 (2013) 12148.
23. B.P. Vinayan, S. Ramaprabhu, *J. Mater. Chem. A,* 1 (2013) 3865.
24. L.S. Zhong, J.S. Hu, Z.M. Cui, L.J. Wan, W.G. Song, *Chem. Mater*., 19 (2007) 4557.
25. H.J. Song, L.C. Zhang, C.L. Qu, Y. He, Y.F. Tian, Y. Lv, *J. Mater. Chem.*, 21(2011) 5972.
26. K. Jasuja, V. Berry, *ACS Nano,* 3 (2009) 2358.
27. X.J. Du, D. Jiang, Q. Liu, J. Qian, H.P. Mao, K. Wang, *Talanta,* 132 (2015) 146.
28. T. Gan, J. Sun, S. Cao, F. Gao, Y. Zhang, Y. Yang, *Electrochim. Acta,* 74 (2012) 151.
29. S.L. Yang, G.F. Wang, G. Li, Du, J. J. L.B. Qu, *Electrochim. Acta,* 144 (2014) 268.
30. L.M. Lu, L.P. Wu, W.M. Wang, X.Y. Long, J.K. Xu, H.H. He, *Int. J. Electrochem. Sci.,* 13 (2018) 2126.
31. M. Liu, J. Deng, Q. Chen, Y. Huang, L. Wang, Y. Zhao, Y. Zhang, H. Li, S.Yao, *Biosens. Bioelectron.*, 41 (2013) 275.
32. K.P. Liu, J.P. Wei, C.M. Wang, *Electrochim. Acta,* 56 (2011) 5189.
33. W. Sun, L.F. Dong, Y.X. Lu, Y. Deng, J.H. Yu, X.H. Sun, Q.Q. Zhu, *Sensor. Actuat. B: Chem.*, 199 (2014) 36.
34. L.S. Duan, L.J. Yang, H.Y. Xiong, X.H. Zhang, S.F. Wang, *Microchim. Acta,* 180 (2013) 355.
35. J. Zhou, K. Zhang, J. Liu, G. Song, B.X. Ye, *Anal. Methods,* 4 (2012) 1350.
36. W. Sun, X.Z. Wang, H.H. Zhu, X.H. Sun, F. Shi, G.N. Li, Z.F. Sun, *Actuat. B: Chem.,* 178 (2013) 443.